INTERNATIONAL JOURNAL OF
COASTAL & OFFSHORE ENGINEERING
IJCOE Vol.10/No. 1/Winter 2025 (20-34)

Available online at: www. Ijcoe.org

Investigating the Impact of Distance between Diffusers in Wastewater discharge system for Marine Environmental Protection by Numerical Method

Amirreza Afifeh[1], Mehdi Nezhadnaderi[2]*, Babak Pordel Maragheh[3], Babak Fazli Malidareh[4], Ali Sheykhbahaei[5] and Seyed Mohammad Mousavi[6]

[1)] Department of Civil Engineering, Tonekabon Branch, Islamic Azad University, Tonekabon, Iran. amirrezaafife@gmail.com
*[*2)] Department of Civil Engineering, Tonekabon Branch, Islamic Azad University, Tonekabon, Iran. (Corresponding Author). mehdi2930@yahoo.com.*
[3)] Department of Civil Engineering, Ardabil Branch, Islamic Azad University, Ardabil, Iran. civil_babak2005@yahoo.com
[4)] Department of Civil Engineering, Babol Branch, Islamic Azad University, Babol, Iran. Fazli.babak@babolia.ac.ir
[5)] PhD Candidate in Physical Oceanography at university of Hormozgan/ Iranian National Institute for Oceanography and Atomospheric science, Ali.sheykhbahaei@inio.ac.ir
[6)] Department of Civil Engineering, Tonekabon Branch, Islamic Azad University, Tonekabon, Iran. Mosavi.622@gmail.com

ARTICLE INFO

Article History:
Received: 15 Nov 2024
Accepted: 25 Jan 2025

Keywords:
wastewater discharge site
leachate, mixing area
primary development
angular spreader

ABSTRACT

The rate of initial development and its characteristics play an important role in the design of wastewater discharge into the sea. It is very common to use mixing zone models to estimate the initial gradient. Considering that salty sea water causes environmental damage due to mixing with wastewater discharged from the desalination site into the sea on the coasts, it was determined by modeling the angled channels that distribute the wastewater on the sea floor that the wastewater from the water site The sweetener enters the sea through the angled channels of the spreader and is pulled towards the shore due to the velocity of the current. The lowest density is in the areas between the spreaders, which shows that the promotion system works well and prevents the sedimentation of the effluent on the sea floor and has reduced the density of the effluent. Also, the lowest velocity is in the areas between the spreaders, which shows that the promotion system works well and prevents the sewage from settling on the sea floor.

[1, 5)] MSc
[2)] Associate Professor
[3 to 6)] Assistant Professor

1. Introduction

Multi-port diffusers are often used to dilute industrial effluents to receiving waters characterized by shallow water depth. Examples of these effluents include heated water from power plants located near the ocean or the coast of Great Lakes, sewage effluent from treatment plants discharged into a river or lake, and saltwater runoff from desalination plants. the ocean Concentrated brine from desalination plants is sometimes mixed with lighter heated water from an on-site power plant or treated wastewater from a sewage treatment plant for energy recovery using pressurized delayed osmosis (PRO) or reverse electrodialysis. (RED) Akram et al. 2013; Weiner et al., 2015)
(Shrivastava and Adam, 2019 studied the mixing of tee diffusers in shallow water with cross flow. This paper analyzes the mixing of a tee diffuser discharging into shallow water with the flow. Experiments are performed for tee diffusers of various designs discharging in a crossflow. Dilution measurements are reported and analyzed along with results obtained by previous studies to investigate the effects of various outlet and environmental parameters on dilution. The effect of ambient flow velocity, diffuser length, port distance, port angle with respect to horizontal, ambient depth, distance near the shore and effluent buoyancy on dilution is investigated. Previous investigations have shown different effects of the ambient flow on the dilution of the three-way diffuser, which is characterized by the ratio of the ambient momentum to the discharge momentum. This apparent confusion is resolved by showing that many of the differences can be attributed to the different range of parameters used in the different studies. While most studies have focused on minimum dilution inside the column, dilution measurements at the edge of a regulatory mixing zone are considered in this paper because they are important to meet regulatory requirements. Measurements of centerline and mean flux dilution at the edge of a mixing zone are reported. Recommendations are given for the design of tee diffusers in shallow receiving waters with cross-flow.

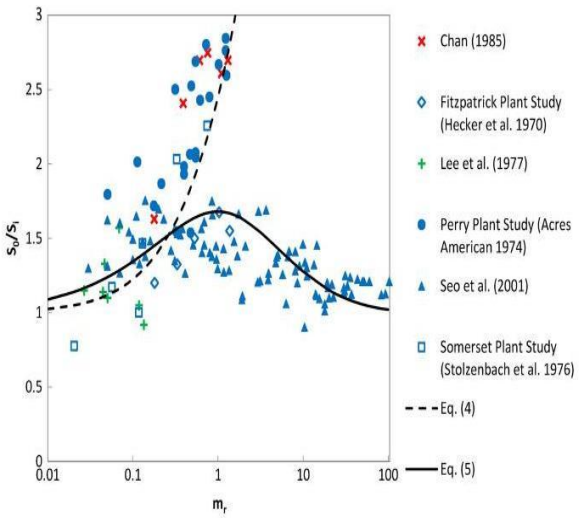

Figure 1- Progressive measurements in areas S1, S2, and S3 for a T-shaped spreader(Shrivastava and Adam, 2019).

Reference	S_0	θ_0 (degrees)	m_r	L/H	l/H	ϕ	Γ
Perry plant study (Acres American 1974)	4–9	0	0.05–1.26	15–75	1–6	0.1–0.3	0
Fitzpatrick plant study (Hecker et al. 1970)	14.9	0	0.18–1.37	30.3	2.5	0.64	1/50
Lee et al. (1977)	7–10	0	0.04–0.14	19–40	0.5–2.5	0–0.2	0
Seo et al. (2001)	10–30	22.5	0.03–104	4–15	0–1	0.1–1.2	0
Somerset plant study (Stolzenbach et al. 1976)	6–15	0	0–0.75	6–34	2	0.2–0.5	1/73.5
Chan (1985)	7.2	0	0.17–1.31	25.4,33.9	0.85	0	0

Figure 2-The parameters used by the previous researchers in the advanced calculation(Shrivastava and Adam, 2019).

Set	Run	L (m)	N	Q_0 (m^3/s)	u_a (m/s)	S_0	m_r	L/H	l/H	ϕ	n	S_3	S_{ave}	L_r
1	1	240	24	25.3	0.07	15.6	0.08	24	1	0.17	2	13.2	—	272
	2	240	24	25.3	0.22	15.6	0.92	24	1	0.17	6	10.6	17.3	272
	3	240	24	25.3	0.52	15.6	4.94	24	1	0.17	2	12.4	23.8	272
	4	240	24	25.3	1.13	15.6	23.29	24	1	0.17	2	15.7	27.6	272
2	5	240	48	25.3	0.06	15.6	0.07	24	0.5	0.17	1	11.2	—	225
	6	240	48	25.3	0.21	15.6	0.81	24	0.5	0.17	1	9.0	—	225
	7	240	48	25.3	0.48	15.6	4.27	24	0.5	0.17	1	10.2	19.6	225
	8	240	48	25.3	0.63	15.6	7.26	24	0.5	0.17	1	11.1	—	225
	9	240	48	25.3	1.05	15.6	20.16	24	0.5	0.17	1	12.9	21.8	225
3	10	240	12	25.3	0.07	15.6	0.08	24	2	0.17	2	14.2	—	267
	11	240	12	25.3	0.22	15.6	0.92	24	2	0.17	2	11.1	—	267
	12	240	12	25.3	0.52	15.6	4.94	24	2	0.17	2	11.2	—	267
	13	240	12	25.3	1.13	15.6	23.29	24	2	0.17	2	15.5	—	267
4	14	240	6	25.3	0.07	15.6	0.08	24	4	0.17	4	13.0	—	242
	15	240	6	25.3	0.22	15.6	0.92	24	4	0.17	3	9.5	—	242
	16	240	6	25.3	0.52	15.6	4.94	24	4	0.17	3	8.7	—	242
	17	240	6	25.3	1.13	15.6	23.29	24	4	0.17	2	11.6	—	242
5	18	300	30	25.3	0.07	17.4	0.10	30	1	0.18	2	14.1	—	245
	19	300	30	25.3	0.22	17.4	1.16	30	1	0.18	2	9.9	—	245
	20	300	30	25.3	0.52	17.4	6.15	30	1	0.18	4	10.1	17.7	245
	21	300	30	25.3	1.13	17.4	29.13	30	1	0.18	2	13.8	24.7	245
6	22	160	16	25.3	0.07	13.1	0.06	16	1	0.15	2	13.3	—	273
	23	160	16	25.3	0.22	13.1	0.59	16	1	0.15	2	10.4	—	273
	24	160	16	25.3	0.52	13.1	3.29	16	1	0.15	2	10.5	—	273
	25	160	16	25.3	1.13	13.1	15.53	16	1	0.15	2	15.0	—	273

Figure 3- Parameters used in advanced calculation (Shrivastava and Adam, 2019).

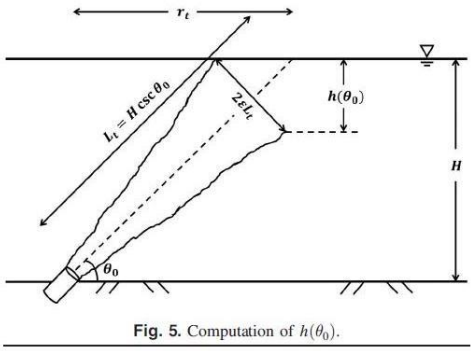

Fig. 5. Computation of $h(\theta_0)$.

Figure 4- Parameters used in advanced calculation (Shrivastava and Adam, 2019).

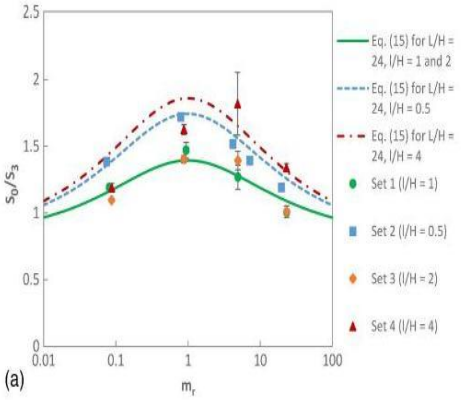

Figure 5- The parameters used in the progress calculation for 6 plans for different *l*/(H) (Shrivastava and Adam, 2019).

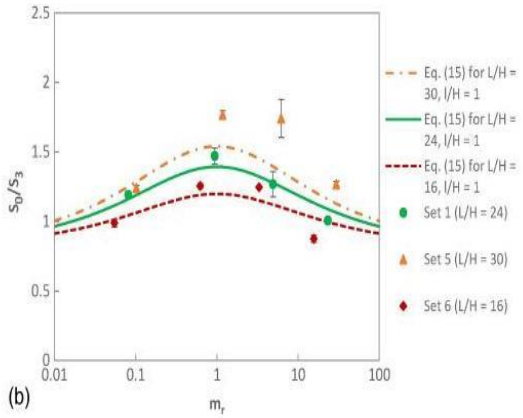

Figure 6- The parameters used in the progress calculation for 6 designs for different L/(H) (Shrivastava and Adam, 2019).

ε ≈ 0.1 is the expansion rate of the half-width jet (Lee and Chu, 2003). h(θ_0) is less than water depth for θ_0 > 11.3 degrees. Therefore, the dilution ratio for a diffuser with horizontal ports relative to ports inclined at an angle θ_0 for θ_0 > 11.3) is as follows:

$$\frac{S(0^{\circ})}{S(\theta_0)} = \sqrt{\frac{A(0^{\circ})}{A(\theta_0)}} = \sqrt{\frac{HL}{lh(\theta_0)}} = \frac{1}{\sqrt{2\varepsilon cot\theta_0}}$$

S1 = ratio of flow induced from behind the diffuser to the
discharge flow rate for a tee diffuser in crossflow;
S2 = minimum dilution within the plume for a tee diffuser in
crossflow;
S3 = minimum dilution at the edge of a mixing zone for a tee
diffuser in crossflow;
A = cross-sectional area occupied by the diffuser plume;
a0 = individual port area;
B = width of effluent plume as it crosses the mixing zone;
b0 = kinematic buoyancy flux per unit length of discharge
effluent;
cd = empirical drag coefficient for tee diffuser in crossflow;
D0 = port diameter;
F0 = densimetric Froude number;
g = acceleration due to gravity;
g00 = reduced gravity of effluent discharging from the outfall;
H = ambient water depth;
hθ0 = water depth occupied by the plume when it hits the
water surface;
L = length of diffuser;
Lm = characteristic length scale for the diffuser;
Lr = ratio of length in the prototype to length in the model;
Lt = length of trajectory till the plume hits the water surface;
l = spacing between ports;
ma = kinematic momentum flux per unit length of the ambient crossflow;
mr = momentum ratio, a nondimensional parameter characterizing the effect of ambient current;
m0 = kinematic momentum flux per unit length of discharge effluent;
N = number of ports;
n = number of replicates for each experimental run;
Q = flow induced by the discharge;
Q0 = flow rate of discharge effluent;
R = jet Reynolds number;
rt = horizontal distance of the point of surface impact from the jet;
S = diffuser dilution;
S ave = flux-averaged dilution at the edge of a mixing zone for atee diffuser in crossflow;
S0 = theoretical dilution of a tee diffuser in quiescent ambient;
ua = ambient current speed;
ud = speed of the plume perpendicular to the mixing zone boundary;
ue = average velocity of the flow being entrained into the diffuser plume;
uf = average velocity of the induced flow in front of the diffuser;
u0 = exit velocity through a port;
xs = distance of the diffuser from the nearshore;
Γ = bottom slope in the offshore direction;
Δρ = density difference between discharge effluent and ambient water;
ε = rate of increase of the jet half-width;
θ = local value of plume inclination relative to horizontal;
θ0 = angle of port inclination with horizontal;
ν = kinematic viscosity of water;
ρa = density of ambient water;
ρ0 = density of discharge effluent;
σ = contraction in the width of the plume discharged from a
tee diffuser; and
ϕ = nondimensional shallowness parameter.

$$\frac{S_t}{S_0} = 1 - C_d m_r$$

$$m_r = \frac{{U_a}^2 H}{{U_0}^2 B}$$

$$B = \frac{A}{l}$$

$$S_0 = \sqrt{\frac{H cos\theta_0}{2B}}$$

$$\frac{S_t}{S_0} = (1 + 5m_r)^{-1/2}$$

In 2017, Absi investigated how to discharge wastewater through angular ducts with the help of laboratory models. There have been extensive reports of dense gradient jets typical of brackish water discharge into shallow water. Experiments were performed with nozzles at 30, 45, and 60 degrees to the horizontal direction, and the spatial changes of restoration concentrations were measured by three-dimensional laser fluorescence (3DLIF). Three flow regimes are known: deep water, surface contact and shallow water. The regimes depend on the value of dF/H, where d is the nozzle diameter, F is the dense mass number of the jet, and H is the water depth; Criteria for transitioning between them are provided. Flow images showed three-dimensional interactions with the free surface, especially for steep nozzle angles in shallow water. The drop in critical points and their locations were measured. For deep water, all results followed those previously reported for fully submerged jets. As the depth (or increase in dF/H) decreases to surface contact, dilutions begin to decrease. Tracer concentration profiles are reduced at the water surface and resemble semi-Gaussian profiles similar to wall jets in shallow water. The jets can stick to the water surface, although the impact point locations and near-field length are not significantly affected by the water surface. In deep water-surface contact regimes, the impact point and near-field dilutions are higher for 60° nozzles. However, the depth decreases, but the dilution is almost equal for the three nozzle angles, until for shallow water, the 30° nozzle leads to a slightly higher dilution. A 30° discontinuity may be preferred for this case because the interaction surface is lower and therefore has less visual effect than the water surface. The previous recommendations that dense jets are located underwater, so that the height of the upper boundary to the jet is less than 75% of the water depth to avoid surface effects seems to be too conservative and the current results show which increase can be up to 90% of water depth for all angles without detrimental effect on dilution.

In 2017, Alden designed the wastewater discharge facility for the Huntington Beach desalination site. Suggested publisher goals (Alden 2017) are to maintain a underground sewers that do not tolerate water table and reduce low amounts of ocean salinity water, requiring discharge shall not exceed a daily maximum of 2.0 ppt above natural sodium not more than 100 meters horizontally from any point of discharge.

The ports are spaced to ensure proper flow between the jets and deliver a horizontal vertical motion of the bay to the dump.

Segregation analysis of this design published by Poseidon was performed using CORMIX (Jenkins, 2017a). This analysis is discussed below. Four flow scenarios are considered: worst case #1 and worst case #2 with temperature difference between effluent and seawater at 0°C and +2°C. To illustrate the methods calculated in R2018, we consider here only the worst case number 1 with a temperature difference of 2 °C (here WC1). The conclusion should be similar for other cases.

Donker and Jirka published a manual for using CORMIX software.

In 2017, Jenkins conducted a hydrodynamic study of a 3D designed model of channel spreaders at Huntington Beach.

(Adams, 1982) derived the progressive equation and angular diffuser using Bernoulli's equations and momentum equation for pressure continuity along the axis of the diffuser. In the case of the angled diffuser, the momentum drop that existed due to the stagnation of the surrounding flow in the momentum equation between the back and front section of the diffuser was taken into consideration. Then, by combining the energy equations and the momentum equations, he calculated the rate of promotion in the area near the discharge for angled diffusers.

The present invention relates to a multiport submerged cooling water discharge diffuser and, in particular, to a diffuser in which the direction of the cooling water discharge is variable as a function of the position of the water discharge relative to the longitudinal center of the diffuser as well as half the length of the diffuser.

When the wastewater is discharged into the sea, the initial mixing of an area with a radius of about 100 meters is done after the wastewater is discharged into the environment through the spreader, which is called the near field. It moves and is spread by the turbulence of this environment, which is called the far field. becomes

For brines, because it has a higher density than sea water and there is a possibility of settling on the bed. Therefore, the discharge of brine should be in such a way that it creates a jet state in the water at the beginning of the discharge so that it can move in the surrounding water and by creating more disturbance in the environment, it causes the mixing of the brine

with the surrounding water to accelerate the progress of the brine and before it drops. The speed and settling of that concentration should be reduced to such an extent that it cannot be separated from the surrounding environment. It should be noted that based on the standards provided by the US Environmental Agency, this process should be carried out within a maximum radius of 200 meters from the sewage discharge location (Moshirpanahei et al., 2019).

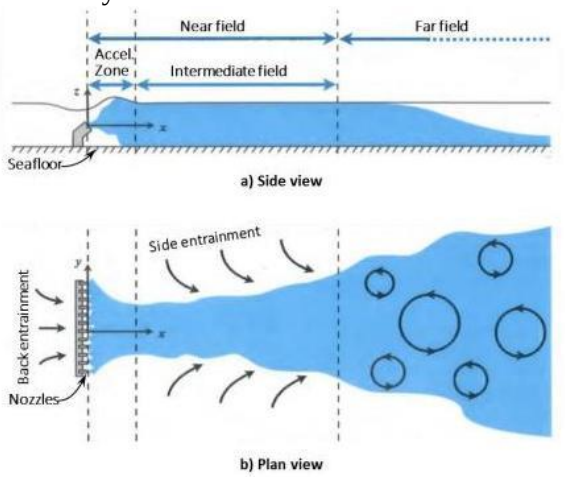

Figure 8- The output flow from the diffuser in the side views and plan modeled in Cormix software (Robert, 2018).

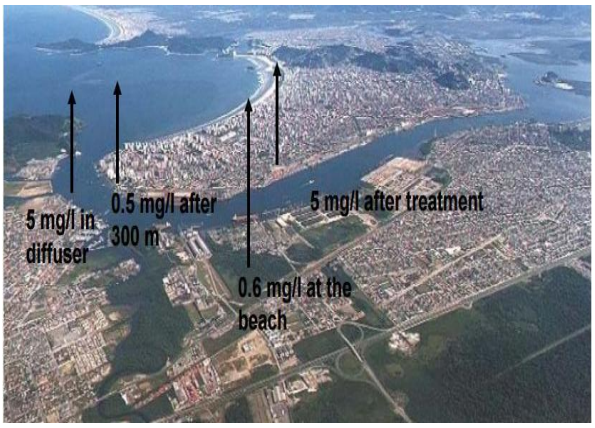

Figure 9- Areas investigated for the management of water quality protection of the effluent discharge environment (Jirka, 2003 and 2004).

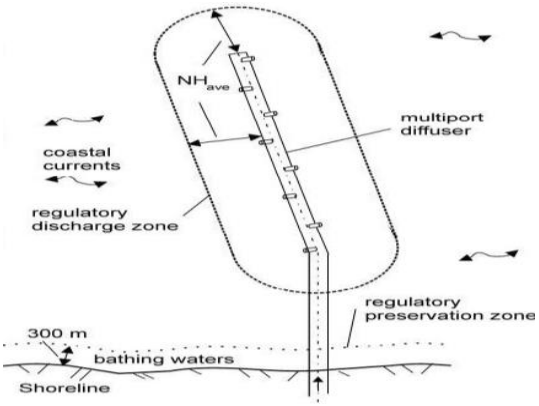

Figure 10- Proposed plan to improve the condition of the investigated areas for the management of water quality protection of the effluent discharge environment (Jirka, 2003 and 2004).

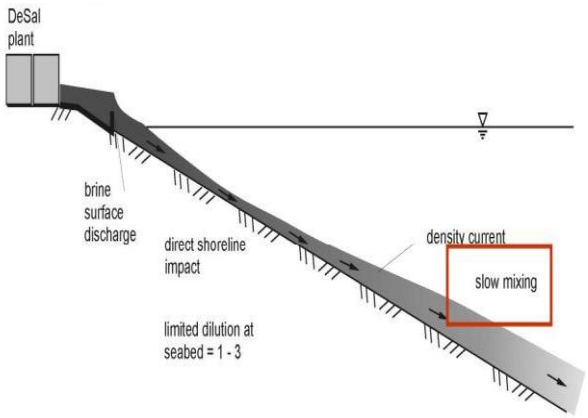

Figure 11- The effect of the output density of wastewater discharge from the RO desalination system (Jirka, 2003 and 2004).

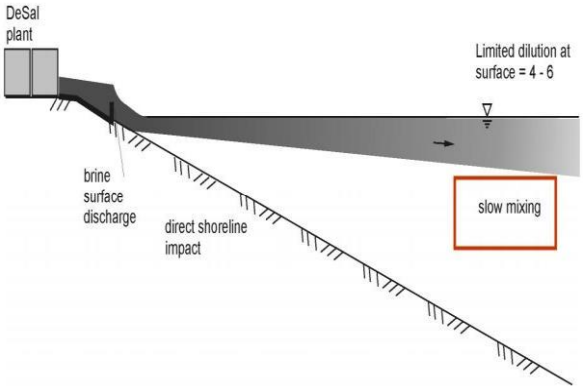

Figure 12- The effect of the temperature of the effluent from the thermal desalination system (Jirka, 2003 and 2004).

Figure 13- Effluent from the discharge of effluents from the surface desalination system in Ashkelon (Jirka, 2003 and 2004).

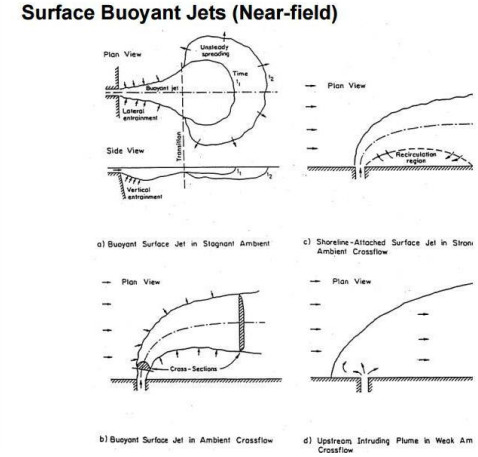

Figure 14- Effluent from the discharge of wastewater from the desalination system in the form of jet flow (Jirka, 2003 and 2004).

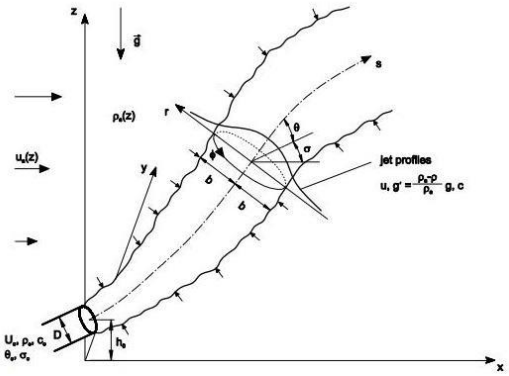

Figure 15- Effluent from the discharge of wastewater from the desalination system in the form of jet flow (Jirka, 2003 and 2004).

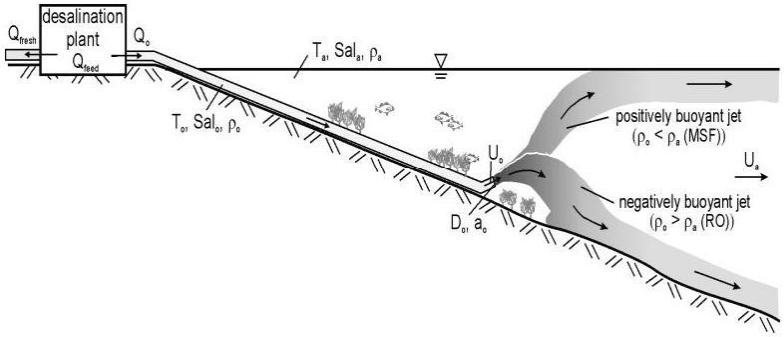

Figure 16- Effluent from the discharge of wastewater from the desalination system in the form of jet flow (Jirka, 2003 and 2004).

Figure 16- Effluent from surface water desalination system in Kuwait (Jirka, 2003 and 2004).

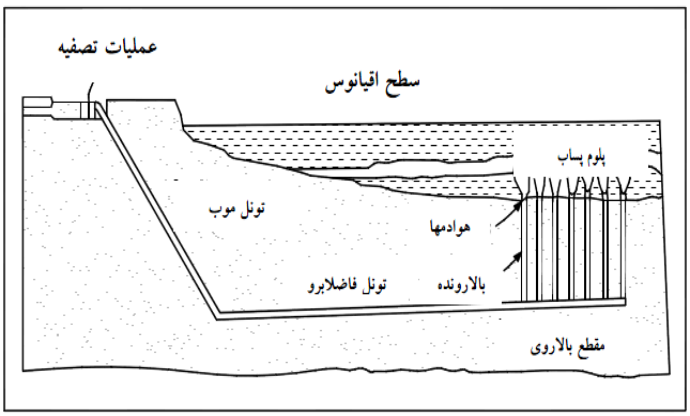

Figure 17- A type of sewage on a tunnel to discharge sewage into sea water (Takdestan et al., 2015).

(Adams, 2014) obtained the progressive equation and angular diffuser using Bernoulli's equations and momentum equation for pressure continuity along the axis of the diffuser.

S_t/S_O=1-$C_d\ M_r$ (۱)

where S_t is the minimum surface elevation for angled diffusers, C_d is the coefficient related to the influence of the stillness of the surrounding flow and M_r is the ratio of the momentum of the surrounding flow to the discharge momentum, which is calculated as follows:

$$M_r = \frac{(U_a)^2 H}{(U_O)^2 D} \quad (2)$$

In this formula, H is the discharge depth, D is the diameter of the discharge channel, Ua is the surrounding flow velocity, and Uo is the discharge velocity. So is the rate of advancement in the surrounding flow at rest, which is presented as follows by (Adams, 2014):

$$S_0 = \sqrt{\frac{H\cos\theta_0}{2B}} \quad (۳)$$

θ_0 is the angle between the channel and the sea floor, which is usually chosen less than 45 degrees.

(Subramania and Puri, 1984) proposed an exponential function based on three-dimensional experiments of a jet in a transverse flow.

(Van Su et al., 2012) obtained the constant coefficients related to the equation by fitting the experimental data as follows:

$$\frac{S_t}{S_o} = \frac{1}{1-[60\exp(-5{M_r}^{0.2})]M_r} \quad (4)$$

By replacing equation (3) in equation (4), we will have:

$$S_t = [1 - [60\exp(-5{M_r}^{0.2})]M_r]\sqrt{\frac{H\cos\theta_0}{2B}} \quad (۵)$$

First, it is necessary to define a parameter for the players. This parameter, which we denote by the letter B, is the ratio of the cross-sectional area of each of the holes of the diffuser to the distance between the holes along the length of the diffuser:

$$B = \frac{A_0}{l} \quad (۶)$$

2. Methods

One of the most important parts of the desalination site is the wastewater disposal system. The importance of this issue is due to both the environmental effects and the economic costs of the project. If the length of the sewage transmission line into the sea is calculated even if it is a few tens of meters extra, considering that the implementation of this transmission line is in the depths of the sea, it will increase the financial burden to the project owner. The rate of initial development and its characteristics play an important role in the design of wastewater disposal into the sea. It is very common to use mixing zone models for initial progressive estimation. In this study, the performance of the distance between diffusers in shallow waters is discussed using hydrodynamic relationships.

Table 1- Environmental parameters of desalinated water

$3\frac{m}{s}$	flow rate
$2\frac{m}{s}$	wind speed
40°C	ambient temperature
0.04	Weissbach Darcy coefficient near the coast
0.13	Weissbach's Darcy coefficient at the point of discharge
4%	Slope near the beach
1.2%	Slope at the discharge site
$45000\frac{mg}{lit}$	Concentration in the environment

Table 2-The characteristics of the multi-channel desalination device

20cm	Pipe diameter
۹	The number of evacuees

Navier-Stokes equations:

$$\frac{\partial \mathrm{U_i}}{\partial \mathrm{X_i}} = 0 \quad (۷)$$

$$\frac{\partial U_i}{\partial t} + U_j \frac{\partial U_i}{\partial \mathrm{X_j}} = -\frac{1}{\rho_r}\frac{\partial P}{\partial \mathrm{X_i}} + \nu \frac{\partial^2 U_i}{\partial X_j \partial X_j} + g_i \frac{\rho - \rho_r}{\rho_r} \quad (۸)$$

$$\frac{\partial \Phi}{\partial t} + U_i \frac{\partial \Phi}{\partial \mathrm{X_i}} = \lambda \frac{\partial^2 \Phi}{\partial X_i \partial X_i} + S_\Phi \quad (۹)$$

$$\mathrm{U_i}=\overline{\mathrm{U_I}}+u_\mathrm{i} \quad ، \quad \mathrm{P}=\bar{P}+\mathrm{p} \quad ، \quad \Phi = \bar{\Phi} + \varphi \quad (۱۰)$$

$$\overline{U_I} = \frac{1}{t_2-t_1}\int_{t_1}^{t_2} U_i dt \quad , \bar{P} = \frac{1}{t_2-t_1}\int_{t_1}^{t_2} P dt \quad , \quad \bar{\Phi} = \frac{1}{t_2-t_1}\int_{t_1}^{t_2} \Phi dt \tag{1}$$

$$\frac{\partial U_i}{\partial X_i} = 0 \tag{2}$$

$$\frac{\partial U_i}{\partial t} + U_j \frac{\partial U_i}{\partial X_j} = -\frac{1}{\rho_r}\frac{\partial P}{\partial X_i} + \frac{\partial}{\partial X_j}\left(\nu \frac{\partial U_i}{\partial X_j} - \overline{u_i u_j}\right) + g_i \frac{\rho-\rho_r}{\rho_r} \tag{3}$$

$$\frac{\partial \Phi}{\partial t} + U_i \frac{\partial \Phi}{\partial X_i} = \frac{\partial}{\partial X_i}\left(\lambda \frac{\partial \Phi}{\partial X_i} - \overline{\varphi u_i}\right) + S_\Phi \tag{4}$$

$$\frac{\partial(\rho k)}{\partial t} + \mathrm{div}(\rho k U) = \mathrm{div}\left(\frac{\mu_t}{\sigma_k}\,\mathrm{grad}\, k\right) - 2\mu\, E_{ij}.E_{ij} - \rho\varepsilon \tag{5}$$

$$\frac{\partial(\rho\varepsilon)}{\partial t} + \mathrm{div}(\rho\varepsilon U) = \mathrm{div}\left(\frac{\mu_t}{\sigma_\varepsilon}\,\mathrm{grad}\,\varepsilon\right) + C_{1\varepsilon}\frac{\varepsilon}{k}2\mu\, E_{ij}.E_{ij} - C_{2\varepsilon}\,\rho\,\frac{\varepsilon^2}{k} \tag{6}$$

3. Numerical simulation

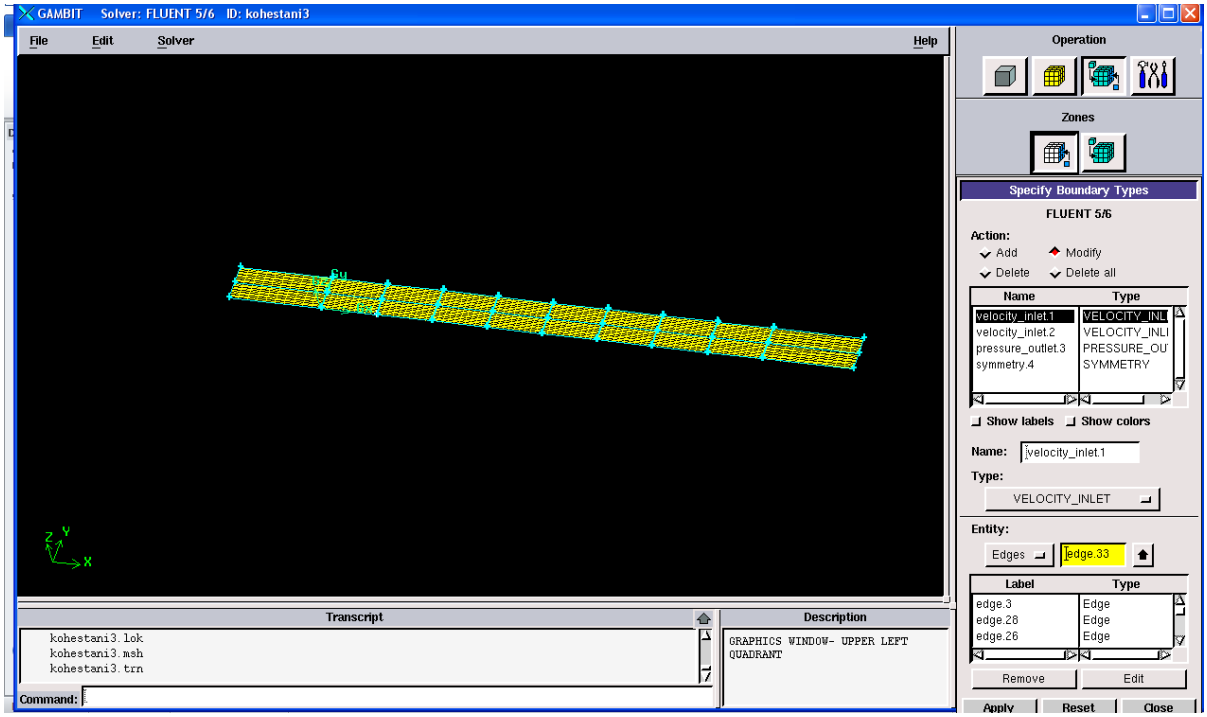

Figure 18- Meshing in Gambit software

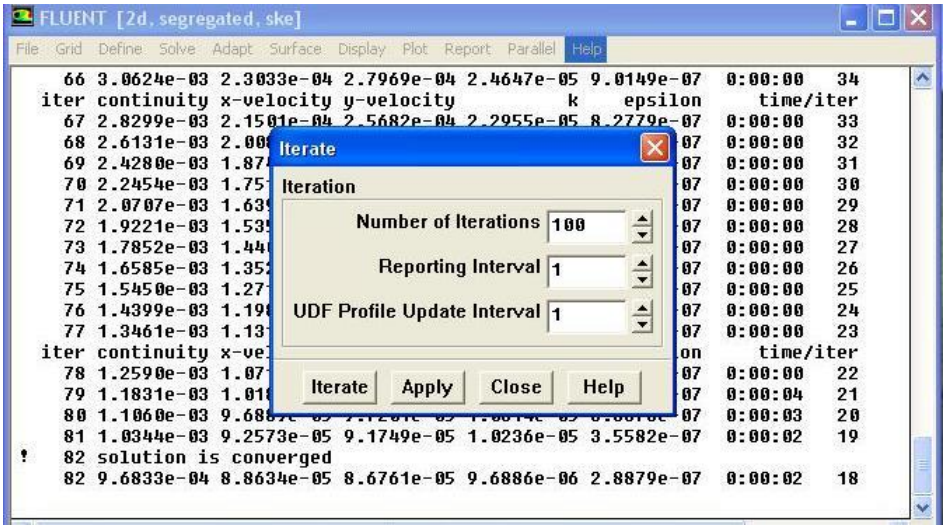

Figure 19- Solving the equations governing the flow in the Fluent environment, which reached convergence after 82 cycles.

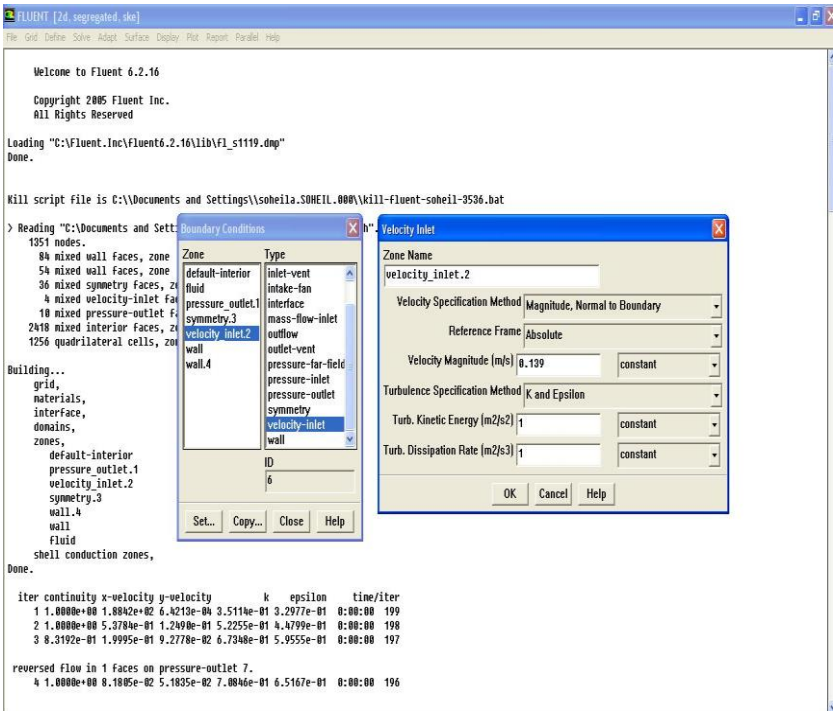

Figure 20- Applying the boundary conditions of the flow velocity in the Fluent environment

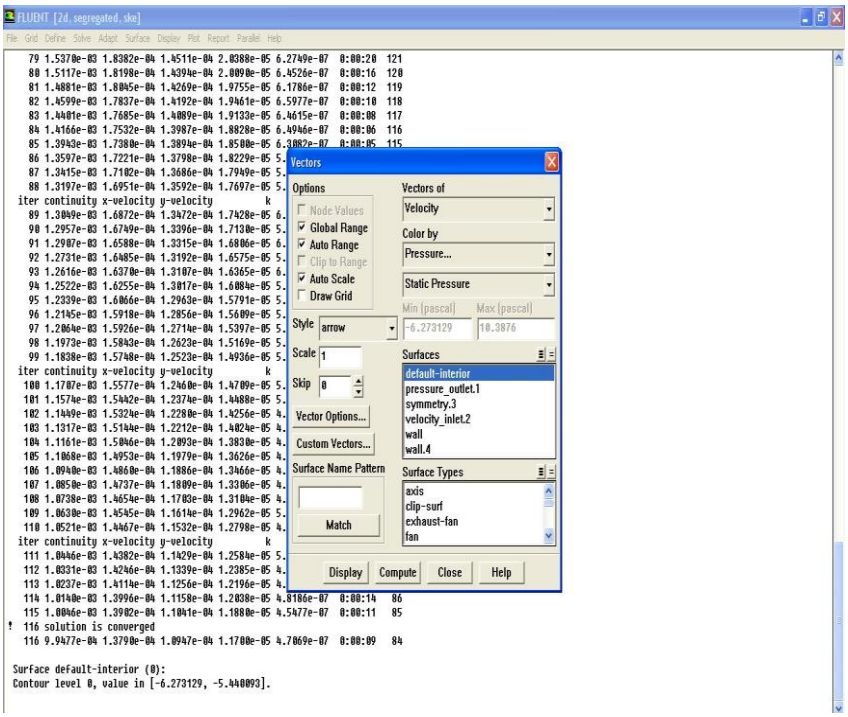

Figure 21-- Reporting the results of solving flow equations in the Fluent environment

According to the information received about the type of water softener system and the introduction of the waste disposal system resulting from it by the multi-duct drainer, considering that the diameter of the ducts is considered to be 20 cm and the distance between the drain holes is 12 meters, the value of B according to the formula (6) is equal to 0.010467. Then, according to the values of H (depth in Table 2-3) and the water velocity in the second column of Table 2-3 and the effluent discharge velocity which is obtained by dividing the effluent flow rate by the outlet cross-sectional area and the outlet diameter, the ratio of the momentum of the surrounding flow to the discharge momentum (M_r) is obtained, also the value of θ_0 is considered equal to 45 degrees. Therefore, the known values are available to find S_t. For the stated scenarios, we obtain S_t.

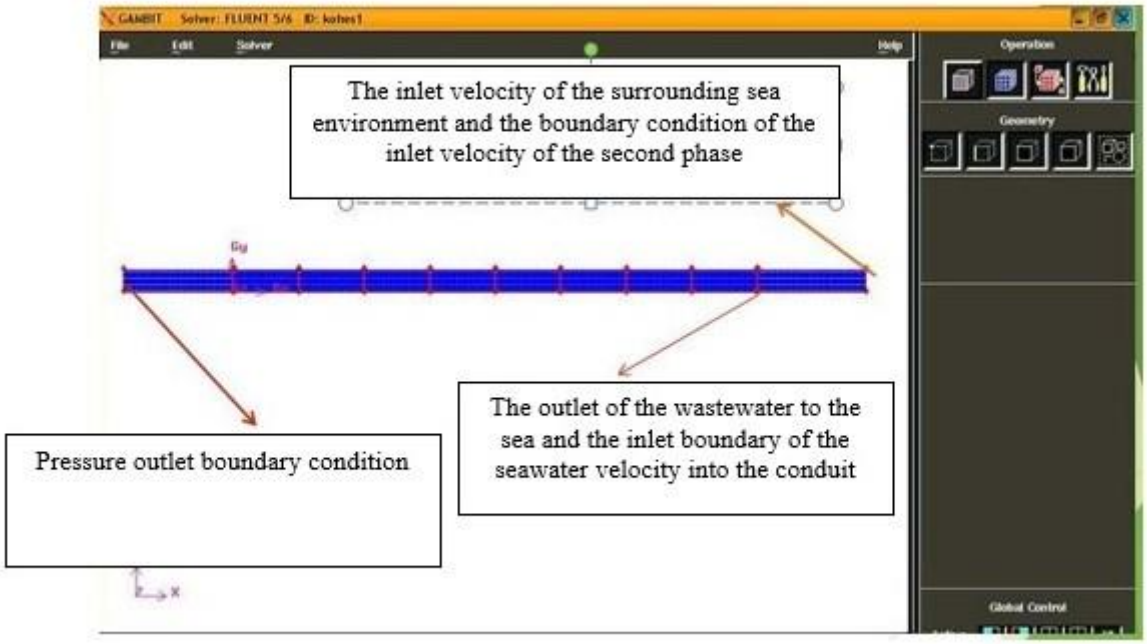

Figure 22- Networking the wastewater flow of the desalination site through the multi-channel system to the sea in Gambit environment

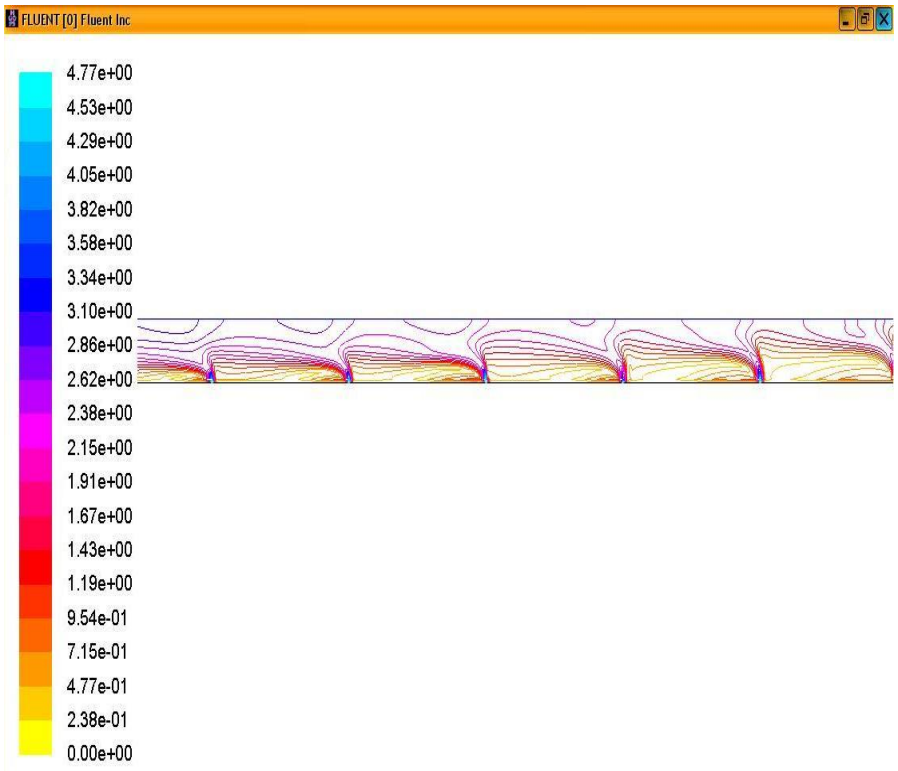

Figure 23- The shape of the iso-velocity curves as a result of the numerical simulation of the effluent flow of the desalination site through the multi-channel system to the sea. The wastewater from the desalination site enters the sea through vertical channels and is dragged to the shore due to the speed of the current. The lowest speed is in the areas between the spreaders, which shows that the promotion system works well and prevents the sewage from settling on the sea floor.

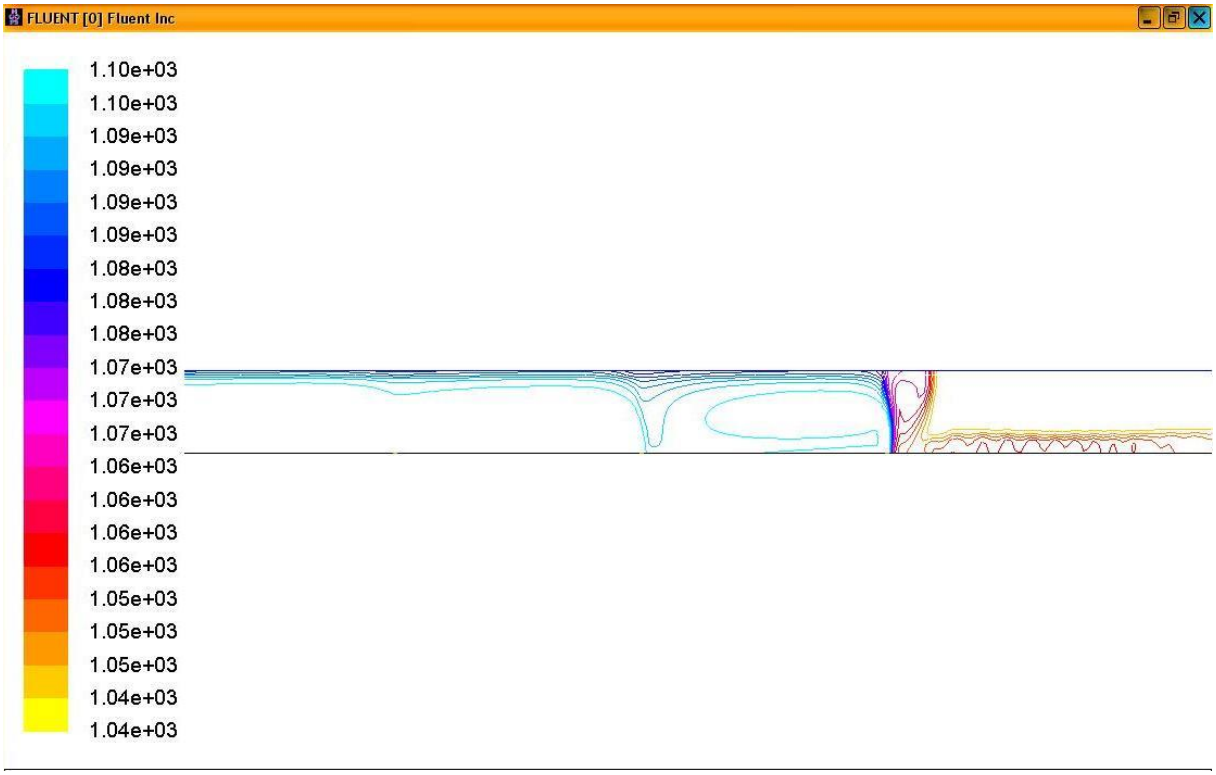

Figure 24- The shape of the density curves as a result of the numerical simulation of the effluent flow of the desalination site through the multi-channel system to the sea. The wastewater from the desalination site enters the sea through vertical channels and is dragged to the shore due to the speed of the current. The lowest density is in the areas between the spreaders, which shows that the promotion system works well and prevents the sewage from settling on the sea floor and has reduced the density of the sewage.

Results

The rate of initial development and its characteristics play an important role in the design of wastewater disposal into the sea. The initial progress depending on the water depth, opening diameter, flow velocity, distance between openings, number of dischargers and ambient water velocity were calculated in this article.

Due to the fact that salty sea water mixed with the wastewater discharged from the desalination site into the sea on the coast causes environmental damage. Using the modeling of the vertical channels for the distribution of wastewater on the sea floor, it was determined that the effluents of the desalination site enter the sea through the angled distribution channels and are drawn towards the shore due to the speed of the current. The lowest density is in the areas between the spreaders, which shows that the promotion system works well and prevents the sewage from settling on the sea floor and has reduced the density of the sewage. Also, the lowest speed is in the areas between the diffusers, which shows that the promotion system works well and prevents the sewage from settling on the sea floor.

References

1. Akram, W., M. H. Sharqawy, and J. H. Lienhard. 2013. “Energy utilization of brine from an MSF desalination plant by pressure retarded osmosis.” In Proc., IDA World Congress on Desalination and Water Reuse. Topsfield, MA: International Desalination Association.

2. Weiner, A. M., R. K. McGovern, and J. H. Lienhard. 2015. “Increasing the power density and reducing the levelized cost of electricity of a reverse electrodialysis stack through blending.” Desalination 369: 140–148.

3. Ishita Shrivastava and E. Eric Adams, M. 2019. Mixing of Tee Diffusers in Shallow Water with Crossflow: A New Look. Journal of Hydraulic Engineering . Volume 145 Issue 4 - April 2019.

4. Lee, J. H. W., and V. H. Chu. 2003. “Turbulent jets and plumes—A Lagrangian approach.” Chap. 2 in Turbulent jets, 36–37.

Dordrecht, Netherlands: Kluwer Academic Publishers.

5. Abessi, O., and Roberts, P. J. W. (2015). "Dense jet discharges in shallow water." J. Hydraul. Eng. 10.1061/(ASCE)HY.1943-7900.0001057.

6. Adams, E. E. (1982). "Dilution Analysis for Unidirectional Diffusers." J. Hydr. Div., ASCE, 108(HY3), 327-342.

7. Alden (2017). "Huntington Beach desalination facility discharge diffuser design." Alden Research Laboratory, Holden, Massachusetts. Memorandum February 23, 2017. H1.pdf.

8. Doneker, R. L. and Jirka, G. H. (2017). "CORMIX User Manual." MixZon, Portland, Oregon. Updated February 2017.

9. Cornell (2014). "Status Report 1 Outfall Redesign Study." SPDES Number NY0244741 Cornell University, Department of Energy & Sustainability, December 22, 2014.

10. Fischer, H. B., List, E. J., Koh, R. C. Y., Imberger, J., and Brooks, N. H. (1979). Mixing in Inland and Coastal Waters, Academic Press, New York.

11. Jenkins, S. A. (2017a). "Alternative Hydrodynamic Model Analysis of the Alden Designed 3-Port Duckbill Diffuser Retrofit at Huntington Beach Desalination Facility (HBDF)- Version 2." Michael Baker International. 29 November 2017. Appendix KKKK3 - Michael Baker Dilution Analysis CORMIX Model Update 2017.11.29 FINAL.pdf

12. Jenkins, S. A. (2017b). "Taylor Micro-Scale Methods for Estimating Injury and Mortality to Marine Organisms Entrained by a Diffuser at Huntington Beach Desalination Facility (HBDF). Michael Baker International. 7 December 2017. Appendix WWWW - Memo - HBDF Turbulence Impact Assessment 2017.12.07 FINAL.pdf

13. Jenkins, S. A. (2018) "Design Evolution of a Diffuser Retrofit at Huntington Beach Desalination Facility (HBDF)." Memorandum submitted to Poseidon Resources, 16 January 2018.

14. Roberts, P. J. W. (2018). "Brine Diffusers and Shear Mortality." Final Report. Prepared for Eastern Research Group, February 2018.

15. Jirka, G. (1982). "Multiport diffusers for heat disposal." J. Hydr. Div., ASCE, 108(HY12), 1425-1468.

16. Jirka, G. H., and Harleman, D. R. F. (1979). "Stability and Mixing of a Vertical Plane Buoyant Jet in Confined Depth." J. Fluid Mech., 94(2), 275-304.

17. Subramanya, K., and Porey, p.d. Trajectory of a turbulent cross. j.hydr.res 2008; Vol(22(5): 343- 345).

18. Won Seo, I.I., Kim, H.S. , Yu, D. and Kim, D.S. Performance of Tee diffusers in shallow water with cross flow. J. of Hydr Eng 2012; Vol(34: 53-61).

19. Lee, J. H., and Jirka, G. H. (1980). "Multiport diffuser as line source of momentum in shallow water." Water Resources Research, 16(4), 695-708.

20. Takdestan, Afshin; Hajizadeh, Nasser and Jafarzadeh, Nematullah. "Sewage discharge into the sea is a favorable option for urban sewage disposal in coastal areas". 7th International Conference on Coasts, Ports and Marine Structures, Ports and Shipping Organization, Tehran. 1385.
21. *Reynolds, O., 1984. On the dynamical theory of incompressible viscous fluids and the determination of the criterion. Phil. Trans. Roy. Soc. London, 123- 161.*
22. *McGurik, J.J. and Rodi, W., 1978. A depth-averaged mathematical model for the near fluid of side discharge into open- channel flow. Journal of Fluid Mechanics, 864, 761-781.*
23. *Keller, R.J. and Rodi, W., 1988. Prediction of flow characteristics in main channel/floodplain flows. Journal of Hydraulic Research, IAHR, 26(4), 425-441.*
24. *Biglari, B. and Sturm, T.W., 1998. Numerical modeling of flow around bridge abutments in compound channel. Journal of Hydraulic Engineering, ASCE, 124(2), 156-163.*
25. *Gibson, M.M. and Launder, B.E., 1978. Ground effects on pressure fluctuations in the atmospheric boundary layers. Journal of Fluid Mechanics, 86, 491-511.*
26. *Rastogi A. K. and Rodi, W., 1978. Prediction of heat and mass transfer in open channels. Journal of Hydraulics Division, ASCE, 104(3), 397- 420.*
27. *Yakhot V., Orszag S.A., Thangam, S., Gatski, T.B. and speziale, C.G., 1992. Development of turbulence models for shear flows by a double expansion technique. Physics of Fluids A, Vol. 4, No. 7, pp1510-1520.*
28. *Wilcox D.C., 1988. Re-assessment of the scale-determining equation for advanced turbulence models. AIAA Journal, vol. 26, pp. 1414- 1421.*
29. *Versteeg, H.K. and Malalasekera, W., 2007. An Introduction to Computational Fluid Dynamics: The Finite Volume Method, Prentice Hall, Feb 16, 503 pages.*
30. *Soltani, M.V. and Rahimi Asl, R., 2003. Computational fluid dynamics by Fluent software, Tehran, Tarrah issues.*
31. Fluent 6.2 User's Guide, Janurary 2005.
32. Gambit 2.2 User's Guide, September 2004.